NRC Research Press

ARTICLE

Assessing responses of *Betula papyrifera* to climate variability in a remnant population along the Niobrara River Valley in Nebraska, U.S.A., through dendroecological and remote-sensing techniques

E. Bumann, T. Awada, B. Wardlow, M. Hayes, J. Okalebo, C. Helzer, A. Mazis, J. Hiller, and P. Cherubini

Abstract: Remnant populations of *Betula papyrifera* Marshall have persisted in the Great Plains after the Wisconsin Glaciation along the Niobrara River Valley, Nebraska. Population health has declined in recent years, which has been hypothesized to be due to climate change. We used dendrochronological techniques to assess the response of *B. papyrifera* to microclimate (1950–2014) and the normalized difference vegetation index (NDVI) derived from satellite imagery (Landsat 5 TM (1985–2011) and MODIS (2000–2014)) as a proxy for population health. Growing-season streamflow and precipitation were positively correlated with raw and standardized tree-ring widths and basal area increment increase. Increasing winter and spring temperatures were unfavorable for tree growth, while increasing summer temperatures were favorable in the absence of drought. The strongest predictor for standardized tree rings was the Palmer Drought Severity Index, suggesting that *B. papyrifera* is highly responsive to a combination of temperature and water availability. The NDVI from the vegetation community was positively correlated with standardized tree-ring growth, indicating the potential of these techniques to be used as a proxy for ex situ monitoring of *B. papyrifera*. These results aid in forecasting the dynamics of the species in the face of climate variability and change in both remnant populations and across its current distribution in northern latitudes of North America.

Key words: paper birch, tree rings, riparian, MODIS, Landsat, NDVI, water, temperature, Nebraska Sandhills.

Résumé : Des populations reliques de *Betula papyrifera* Marshall ont persisté dans les grandes plaines après la glaciation du Wisconsin le long de la vallée de la rivière Niobrara, au Nebraska. L'état de santé des populations s'est détérioré au cours des récentes années, vraisemblablement à cause des changements climatiques. Nous avons utilisé les techniques dendrochronologiques pour évaluer la réaction de *B. papyrifera* au microclimat (1950–2014), ainsi que l'indice de végétation NDVI dérivé de l'imagerie satellitaire (Landsat 5 TM (1985–2011) et MODIS (2000–2014)) en tant que substitut reflétant l'état de santé des populations. La précipitation et l'écoulement fluvial durant la saison se croissance étaient positivement corrélés avec l'augmentation de l'accroissement de la surface terrière et la largeur brute et standardisée des cernes annuels. L'augmentation des températures hivernales et printanières était défavorable pour la croissance des arbres tandis que l'augmentation des températures estivales était favorable en l'absence de sécheresse. Le meilleur prédicteur pour les cernes annuels standardisés était l'indice de sévérité de la sécheresse de Palmer, ce qui indique que *B. papyrifera* est très sensible à une combinaison de température et de disponibilité de l'eau. L'indice NDVI de la communauté végétale était positivement corrélé à la croissance des cernes annuels standardisés, ce qui indique que ces techniques peuvent être utilisées comme substitut pour le suivi ex situ de *B. papyrifera*. Ces résultats vont aider à prédire la dynamique de cette espèce face aux changements climatiques tant dans les populations reliques que partout dans son aire de répartition actuelle sous les latitudes septentrionales de l'Amérique du Nord. [Traduit par la Rédaction]

Mots-clés : bouleau blanc, cernes annuels, riverain, MODIS, Landsat, indice de végétation NDVI, eau, température, dunes du Nebraska.

1. Introduction

Paper birch (*Betula papyrifera* Marshall) is a widely distributed deciduous tree species across continental North America. It grows in the boreal forest from Newfoundland in eastern Canada all the way to northwestern Alaska (United States), crossing the Canadian prairies in Manitoba, Saskatchewan, and Alberta. *Betula papyrifera* also extends south from Washington in the western United States to Montana and through the Great Lake States to New England in the eastern United States. Scattered populations can be found in the Great Plains of Montana and North Dakota, the Black Hills of South Dakota, the Appalachian Mountains, and the Front Range of Colorado (Burns and Honkala 1990; map: http://nativeplantspnw.com/paper-birch-betula-papyrifera/). As a boreal species, *B. papyrifera* is adapted to

Received 16 May 2018. Accepted 9 November 2018.

E. Bumann, T. Awada, B. Wardlow, M. Hayes, J. Okalebo, A. Mazis, and J. Hiller. School of Natural Resources, University of Nebraska-Lincoln, Lincoln, NE 68583–0961, USA.
C. Helzer. The Nebraska Nature Conservancy, Omaha, NE 68102, USA.
P. Cherubini. School of Natural Resources, University of Nebraska-Lincoln, Lincoln, NE 68583–0961, USA; Swiss Federal Institute for Forest, Snow and Landscape Research, CH-8903 Birmensdorf, Switzerland; Department of Forest and Conservation Sciences, University of British Columbia, Vancouver, B.C., Canada.

Corresponding author: T. Awada (email: Tawada2@unl.edu).

the cold northern climate (Fowells 1965; Stroh and Miller 2009) and has been found to have mixed responses to temperature, especially during the growing season. Warming temperatures in the spring can result in an earlier bud burst, which can have positive impacts on growth due to increased cambial activity when water is available (Karlsson et al. 2004; Hollesen et al. 2015; Li et al. 2016), but this comes with a risk of early season frost, which can damage and kill newly emerging buds and rootlets and may result in crown dieback (Pomerleau 1991). Water availability has also been shown to positively affect the performance of the species (Kharuk et al. 2014; Li et al. 2016). Water stress — including both excess water and drought — can cause defoliation (Wang et al. 2016), leading to suppressed tree-ring growth and performance for up to 4 years following defoliation (Karlsson et al. 2004).

After the Wisconsin Glaciation, remnant stands of *B. papyrifera* have persisted in the Great Plains but with declining presence (Wright 1970; Stroh and Miller 2009). One of these ecotypes is located along the Niobrara River Valley in north-central Nebraska, where the species can be found in north-facing canyons and along riverbanks. The valley plays an important ecological role as an ecotone where grassland and forest species converge, supporting a diverse array of vegetation that is rarely found in close proximity elsewhere (Stroh and Miller 2009). Short grass species from the semi-arid grasslands of the surrounding Sandhills, as well as grasses representing the mixed and tall grass prairies, can be found alongside forest species representing the western coniferous, eastern deciduous, and boreal communities.

On a continental scale, one of the main threats to *B. papyrifera* has been increased climate variability, specifically temperature and precipitation. The species rarely occurs in areas where average July temperature exceeds 21 °C (Stroh and Miller 2009). In comparison, the Niobrara River Valley July average temperature is approximately 23.8 °C. Stroh and Miller (2009) attributed the health of the Niobrara River Valley populations to a cooler localized microclimate and the close proximity to the riverbank. They reported dieback of *B. papyrifera* in recent years, which is thought to have started around the 1980s and is possibly attributed to temperature increase.

Dendrochronological techniques can be applied to investigate ecological processes and tree responses to site conditions, which are then related to tree performance and forest productivity and health (Cherubini et al. 2002). Factors such as site characteristics, abiotic and biotic environment, management practices, species growth habits, and genetics have been reported to influence the formation and growth of tree rings and, thus, forest productivity (e.g., Schweingruber 1996; Di Matteo et al. 2010; Aus Der Au et al. 2018). The normalized difference vegetation index (NDVI) is another tool that is commonly used in remote-sensing applications as a measure of photosynthetic activity, which can then be related to plant health and growth through examining the ratio of spectral reflectance between the red and near-infrared regions of the electromagnetic spectrum (Vicente-Serrano et al. 2016). The few studies that have explored the relationship between NDVI and tree rings in the literature have shown that the relationship depends on vegetation type, spatial scale, period of study, and the abiotic and biotic environments (Bunn et al. 2013; Vicente-Serrano et al. 2016; Bhuyan et al. 2017). While tree-ring studies are important for quantifying long-term variability in forest productivity, preparing the chronologies can be time consuming and costly on a large scale. On the other hand, NDVI provides a good measure for landscape photosynthetic activity and site productivity and can be used to monitor landscape processes on a regular basis. Therefore, investigating how these two techniques relate to each other can improve our understanding of forest growth and productivity, carbon budgets, and forests response to climate variability and change (Bhuyan et al. 2017).

At present, few studies have attempted to correlate tree rings with NDVI (Bhuyan et al. 2017), and even fewer have been conducted on this remnant *B. papyrifera* ecotype (Stroh and Miller 2009). It is unknown how climate fluctuations impact the performance of this species. The aims of this research are to (*i*) use dendrochronological techniques to assess the past responses and performance of *B. papyrifera* to intra- and inter-annual microclimatic variability and (*ii*) determine if satellite imagery can serve as a proxy for assessing tree health by relating vegetation indices such as NDVI to tree-ring characteristics. This study focuses on a time period between 1950 and 2014. Results can have management implications and are important for the development of biogeographical and ecophysiological predictive models aimed at forecasting the dynamics and performance of this species in the face of future climate variability and change in both remnant populations and across its current habitat range in northern latitudes.

2. Materials and methods

2.1. Site selection

The study area was located at the Nature Conservancy's Niobrara Valley Preserve in north-central Nebraska, centered at 42°78′34″N, 100°02′80″W, and encompasses nearly 227 km² (Fig. 1). Seven north-facing *B. papyrifera* stands were selected along a 27 km section of the river. The valley is 60 to 90 m deep and ranges between 0.8 and 3.2 km in width. The water flow in the adjacent Niobrara River and its tributaries is in part determined by groundwater contribution (Szilagyi et al. 2003), as the groundwater flows over bedrock, therefore creating a high water table. Soil type is mostly alluvial fine-grained sand with a small amount of coarser material (Cady and Scherer 1946). Water moves in an easterly direction at a rate of roughly 0.3 $m \cdot d^{-1}$ through aquifers at a downward slope of anywhere from 2.5 to 13 m for every kilometre of easterly travel (Bradley 1956).

Sites were identified visually and accessed via the river by a canoe. *Betula papyrifera* individuals were mostly present close to the river as part of a deciduous woody species community. Individuals were found only on north-facing slopes and growing from pre-existing root crowns. We did not observe any new seedlings or saplings in sites examined. The upland plant community was dominated by coniferous species, including *Pinus ponderosa* Douglas ex P. Lawson & C. Lawson and the native invasive *Juniperus virginiana* L. mixed with grasses. Sites were marked and Global Positioning System (GPS) locations were acquired for all trees (Fig. 1).

2.2. Microclimate

Precipitation and temperature data were acquired from the Ainsworth and Springview weather stations, located less than 35 km away, via the High Plains Regional Climate Center (HPRCC), University of Nebraska-Lincoln (HPRCC, https://climod.unl.edu/). Long-term (1901–2015) annual precipitation ranged between 241 and 938 mm and averaged 572 mm (Figs. 2 and 3). January average minimum and maximum temperatures were –12.3 °C and 0.4 °C, respectively, and July average minimum and maximum temperatures were 16.5 °C and 31.2 °C, respectively (Fig. 3). Monthly and annual Palmer Drought Severity Index (PDSI) data were acquired from NOAA (https://www7.ncdc.noaa.gov/CDO/CDODivisionalSelect.jsp#), calculated for the region of north-central Nebraska. PDSI is effective in determining long-term drought and takes into account potential evapotranspiration (Fig. 2). Monthly streamflow rate was obtained from the U.S. Geological Survey (USGS) National Water Information System (https://waterdata.usgs.gov/nwis/uv/?site_no=06461500&agency_cd=USGS&referred_module=sw), Sparks, Nebraska (station code: 06461500; 42°54′14″N, 100°26′13″W). The stream gauge is located approximately 30 km from the study sites (Fig. 3). USGS uses the information from the gauges for decision-making on water management and as a warning system during extreme weather events.

Fig. 1. Location of the study area along the Niobrara River Valley in north-central Nebraska, U.S.A. Locations of the examined *Betula papyrifera* stands are marked with black dots. [Colour version available online.]

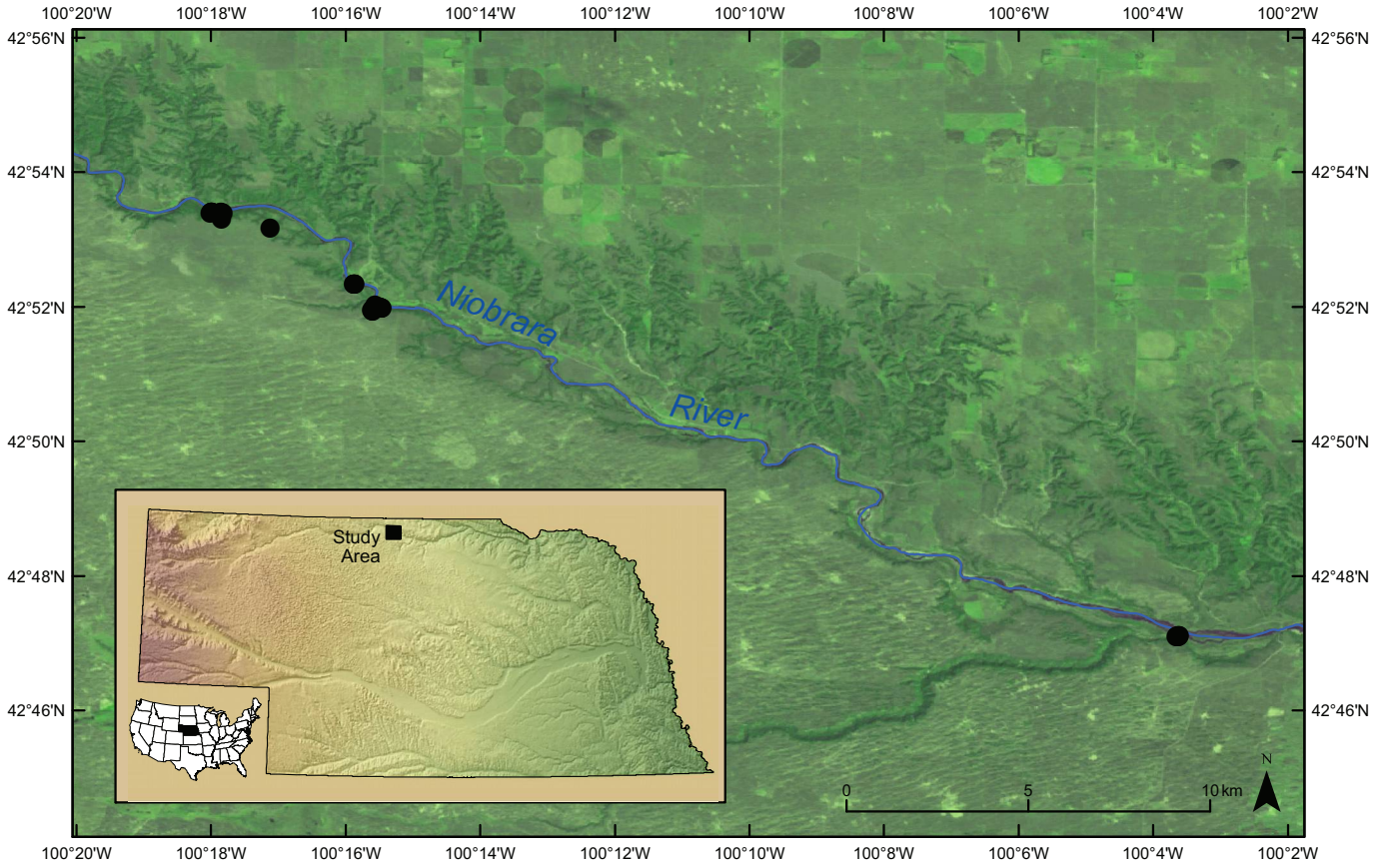

2.3. Tree-ring parameters

We selected the largest trees based on healthiest visual appearance and largest diameter measured at breast height (DBH; Fig. 4). A total of 180 cores, i.e., four cores from each of 45 trees, were sampled at 1.3 m from the base, at 90° around the trunk, representing the north, south, east, and west sides (Maeglin 1979). The oldest ring record dated back to 1894, with the majority of consistent records across trees rings dating back to the early 1950s, thus the time frame selected for this study. Cores were placed on trays, glued to wooden dowels, and sanded flat and smoothed with 150-, 220-, 440-, and 600-grit sandpaper. Cores from southern- and western-facing sides of the trunk were sent to the tree-ring dendrochronological laboratory at the Swiss Federal Institute for Forests, Snow and Landscapes (WSL), Switzerland (the reason for sending half of the samples to WSL was to measure both width and carbon and oxygen isotope ratios in annual tree rings; unfortunately we did not have enough wood material per annual ring to perform the isotope analysis). Northern- and southern-facing cores remained at the Forest Ecophysiology Lab at the University of Nebraska (UNL) where they were scanned at 3200 dpi and individual ring widths were measured to the nearest 100th of a millimetre (0.01 mm) and cross-dated with the Windendro software platform. At WSL, the rings were measured under a microscope to the nearest 0.01 mm using a linear table, "LINTAB" (Rinn 2003). The data were recorded, presented, and analyzed in TSAPWin (Time Series Analysis and Presentation, Frank Rinn, Heidelberg, Germany; Stokes and Smiley 1968; Rinn 2003). After visually cross-dating each tree core (north, south, east, and west), each sample plot was visually cross-dated in TSAPWin. Missing rings were inserted manually with a value of 0 to complete the chronology. The visually cross-dated data were imported into CONFECHA for statistical analysis to check cross-dating accuracy (Grissino-Mayer 2001). Additionally, we determined the "Gleichläufigkeit" (Glk), which is a measure of the year-to-year agreement between the interval trends of two chronologies based upon the sign of agreement and usually expressed as a percentage of cases of agreement (Eckstein and Bauch 1969), as well as the cross-dating index (CDI), which is a combination of the Glk and the *t* value of the chronology (Rinn 2003). Basal area increment (BAI) increase was calculated from raw tree-ring measurements. Raw tree-ring widths were standardized using the "detrendeR" package (Campelo 2012). Input values for the detrending procedure were set to spline length 20 and bandwidth 0.65, $P < 0.05$. Standardization removes biological factors of the individual samples due to age, disturbance, stand density, and size, leaving a value influenced primarily by climate (Cook and Holmes 1986).

2.4. Tree-ring statistical analysis

Statistical analysis was carried out in R using linear mixed modeling through the package "lme4" (Bates et al. 2015). In all models considered, independent variables were represented by monthly cumulative precipitation, monthly average streamflow, monthly (mean, maximum, and minimum) temperatures, and annual PDSI, with year, stand, and sample (tree ID) as random effects. Monthly inclusion began in the growing season of the previous year through October of the current year. All models considered 1950–2014 for the time period, and individual trees were considered as separate response variables. Through early model creation, all parameters of spatial distinction (i.e., slope, aspect, distance and elevation to ridgeline and river edge) were removed as they did not show any statistical significance. They were thus not considered in the creation of final models.

Fig. 2. Annual precipitation, average air temperature, streamflow, and Palmer Drought Severity Index (PDSI) for the study area along the Niobrara River Valley in north-central Nebraska. Dashed lines describe the parameter trend over time.

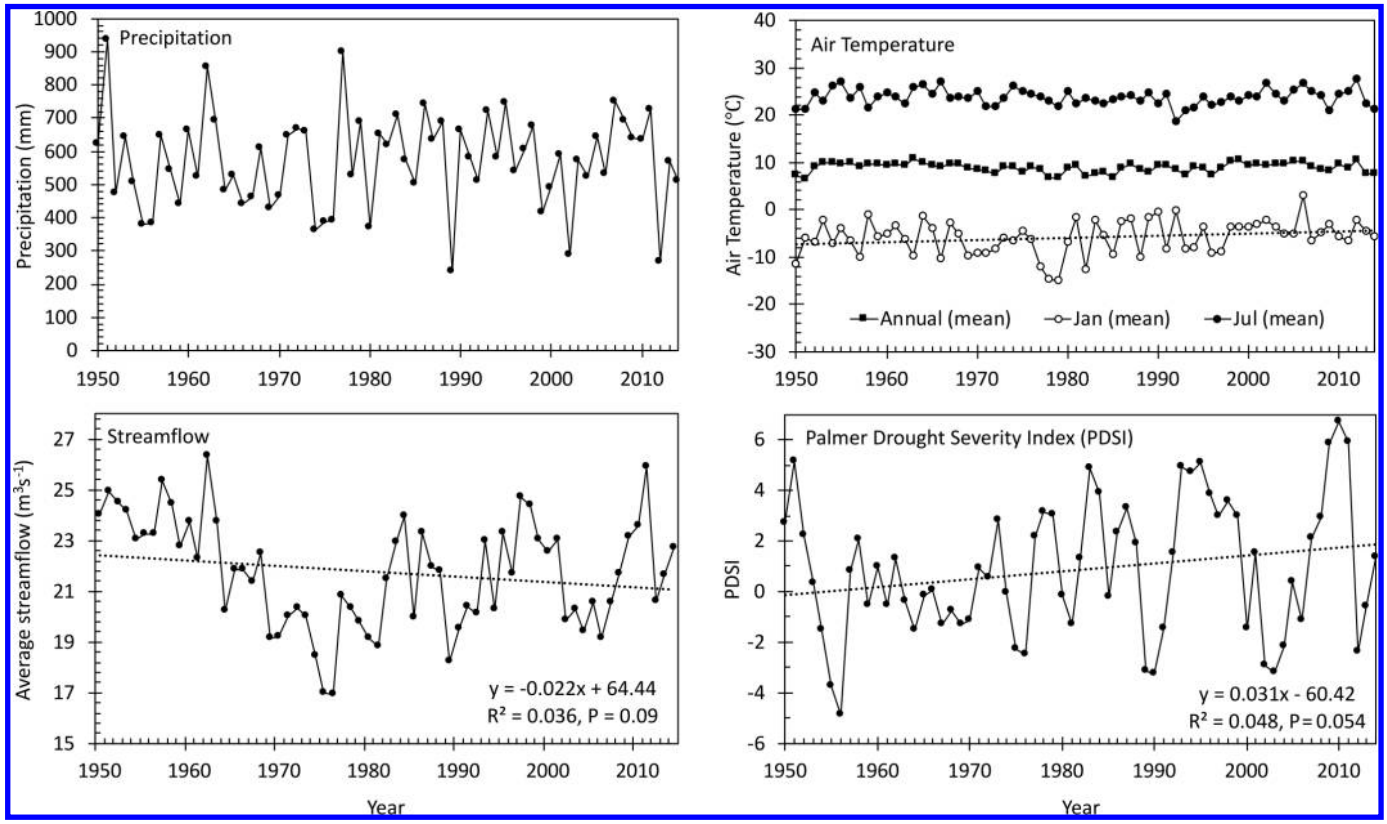

Fig. 3. Long-term average monthly streamflow of the Niobrara River ($m^3 \cdot s^{-1}$), air temperature (°C), and precipitation (mm) between 1950 and 2014.

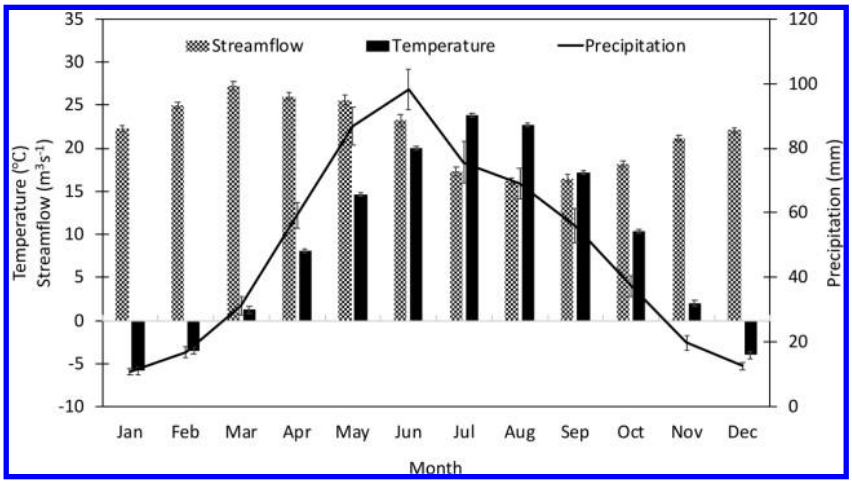

Stepwise backward selection is a process wherein a model is selected by removing one variable at each step of the process based on t statistics of their estimated coefficients (Statistical Consulting Group (UCLA) 2006). It is useful for selecting models from a moderate-sized pool of all potential inclusions. Concerns arise from using this method as variables that are significant to the project at hand may be removed in early selection. When this method is employed, one must give consideration to the legitimacy of the selected product from a real-life perspective (Burnham and Anderson 2002).

All variables for consideration were included in a "global model" from which variables were systematically removed. At every step, all variables were individually tested for inclusion or removal using a χ^2 test based on their P value, and a new model was created using the significant variables ($P < 0.05$). This process was repeated until the highest calculated P value of variable removal was $P < 0.05$. At this point, model selection was complete and the final model was considered determined.

2.5. Landsat and MODIS NDVI image analysis

Landsat 5 Thematic Mapper (hereafter simply "Landsat") offers a spatial resolution (30 m) image with 16-day repeat cycle between image acquisitions and data dating back to the 1980s, which serves as a valuable information source on landscape patterns and conditions over the study area. Landsat-derived NDVI data were used in this study as a proxy of plant health and productivity.

Fig. 4. Diameter at breast height (DBH) as a function of age of *B. papyrifera* trees.

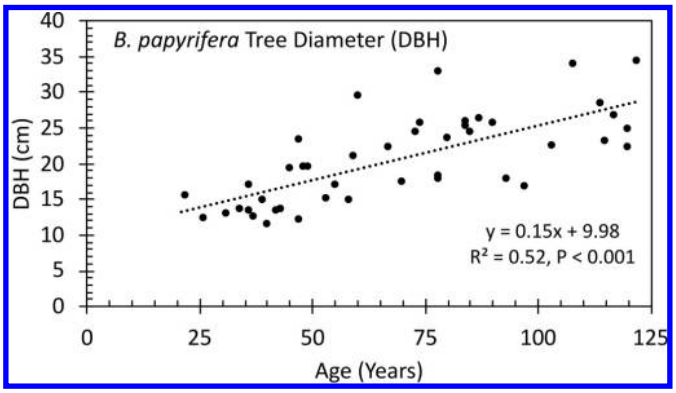

Images were acquired from Google Earth Engine using the "LANDSAT/LT5_L1T_32DAY_NDVI" dataset with the Landsat cloud score algorithm applied to every available scene through the growing season, March through October, from 1985 to 2011. Pixels identified as "cloud" or "primarily water" were removed. The NDVI was calculated as the ratio of reflectance between the red (R, 630–690 nm) and near-infrared (NIR, 760–900 nm) regions of the electromagnetic spectrum as NDVI = (NIR − R)/(NIR + R).

NDVI values fall within the range of –1 to 1. The series of Landsat-based NDVI images available during the March to October time period for each year were temporally stacked for each image pixel. The maximum NDVI value was selected at the pixel level for each individual year to represent a measure of annual productivity. A total of 16 annual, maximum-value NDVI images were produced and compared with annual tree-ring measurements for each corresponding year. Years were excluded if they did not have adequate cloud-free Landsat imagery to calculate maximum NDVI values that could be used in this study. As a result, annual representative images comprised of data from June, July, and August of 1988, 1990–2001, and 2003–2007 were used to create a raster of pixel-based correlation (Pearson's R^2) values against tree-ring widths.

While Landsat images provide a high spatial resolution, the drawback to using it comes by way of cloud obstruction. We applied similar methods for comparison with MODIS imagery, which offers a consistent, high temporal resolution multi-spectral dataset useful for examining surface changes throughout the year with imagery recorded every 1–2 days since December 1999 to present at 250–1000 m pixel resolution. NDVI image data were acquired through Google Earth Engine from the MODIS Terra Daily NDVI (image collection: "MODIS/MOD09GA_NDVI") data set for all available dates between March and October from 2000 to 2014. Cumulative growing season NDVI from MODIS imagery (Reed et al. 1996; Li et al. 2015; Kumar and Mutanga 2017) has been shown to provide a stronger estimate of aboveground biomass and seasonal productivity than single-date NDVI. Summed NDVI through distinct portions of the growing season were also examined and correlated to tree-ring growth. NDVI images were "stacked" for the time periods of March–October (full growing season), March–May (early season), June–August (mid-season), August–October (late season), May, June, July, and August. "Summed NDVI" or "accumulated NDVI values" for each date for these growing season windows within a specific year, which is considered a spectral-based proxy of general vegetation productivity, were correlated using the Pearson's R^2 at the pixel level with tree-ring width.

2.6. Relationships between tree rings and NDVI

Tree-ring chronologies have been shown to reflect a strong, significant correlation with NDVI in other studies (He and Shao 2006; Forbes et al. 2010; Bhuyan et al. 2017). Tree coverage in each stand was smaller than an individual pixel's area in either the Landsat (30 m) or MODIS (250 m) imagery, which resulted in much of the area being comprised of non-*B. papyrifera* land cover types. The landscape position of *B. papyrifera* in remnant populations on steep banks close to the river was an additional reason that the remote-sensing image pixels containing the tree stands could not be directly compared. The stands were located near water, and many of the image pixels containing the tree stands were predominately covered by either water or shade from the steep riverbank. In both cases, the spectral signal and resultant NDVI would be primarily representative of the water and shaded area rather than the actual conditions of the *B. papyrifera*. As a result, direct, pixel-level comparison between the NDVI image pixels and the ground data could not be compared. This required alternative areas of a different land cover type to be used as a productivity proxy to compare with the traditional tree-ring data.

To address this, we investigated whether a relationship between *B. papyrifera* and the pixel-based NDVI signal during the peak growing season could be established with plot-based vegetation in the adjacent community. If successful, this method could then be applied elsewhere to similar areas. The adjacent grasslands were partitioned into eight plots (as shown in Fig. 7), across a series of management areas along the Niobrara Valley Preserve for long-term monitoring. These plots included rotational grazing (plots 1, 2, 3), patch-burn cattle grazing (plot 4), patch-burn cattle grazing, burned in 2015 (plot 5), unburned cattle grazing, control (plot 6), bison grazing, burned in 2015 (plot 7), and bison grazing, unburned (plot 8). In the patch-burn grazed areas, there were no fires in 2016, so the two grids in each site were in unburned areas (for at least several years) versus burned areas in 2015. The patch-burn cattle control site is unburned but grazed season-long at the same stocking rate as the patch-burn cattle pasture. In the rotational grazing treatments, each pasture is grazed at a different time each year.

Each plot consisted of an 8 m × 6 m grid (eight GPS points east–west; six GPS points north–south) encompassed in an area of 640 × 480 m^2. At each GPS point, a 1 m^2 quadrat was dropped and vegetation was sampled. Canopy height and percent cover of each vegetation functional group (grass, shrubs and forbs), as well as litter, standing dead, and bare soil, were recorded. Topography and vegetation composition were considered in reference to pixel-based NDVI and tree-ring growth correlation of *B. papyrifera* to identify potential areas of proxy monitoring based on their vegetation and (or) topographical characteristics. We calculated the Pearson's R^2 value between averaged annual ring growth (raw, standardized, BAI,) and the annual representative NDVI values at each pixel location over the observed area. The R^2 values were organized in a single raster representing the pixel-level correlation to growth.

3. Results

3.1. Site microclimate

Annual cumulative precipitation for the area during the study period of 1950–2014 averaged 573 ± 18 mm. During the 65-year study period, annual precipitation did not show any increasing or decreasing trend over time; instead, precipitation varied annually around the mean (Fig. 2). The majority (80%–90%) of the annual precipitation fell during the growing season between April and September (Fig. 3). Average annual streamflow ranged between 17 and 26.5 $m^3 \cdot s^{-1}$, with a mean annual streamflow of 21.7 ± 0.3 $m^3 \cdot s^{-1}$ (Fig. 3). During the study period, average annual streamflow declined over time, which was significant at $P < 0.1$. Streamflow increased in the spring with snowmelt and declined in July through September with a decrease in precipitation and increases in temperature and evapotranspiration demands, before increasing again in October (Fig. 3). Annual PDSI ranged from –4.9 to 6.7,

Fig. 5. Average annual (A) raw tree-ring width (mm), (B) basal area increment increase (mm²), and (C) standardized ring width (mm) of *B. papyrifera* along the Niobrara River Valley between 1950 and 2014.

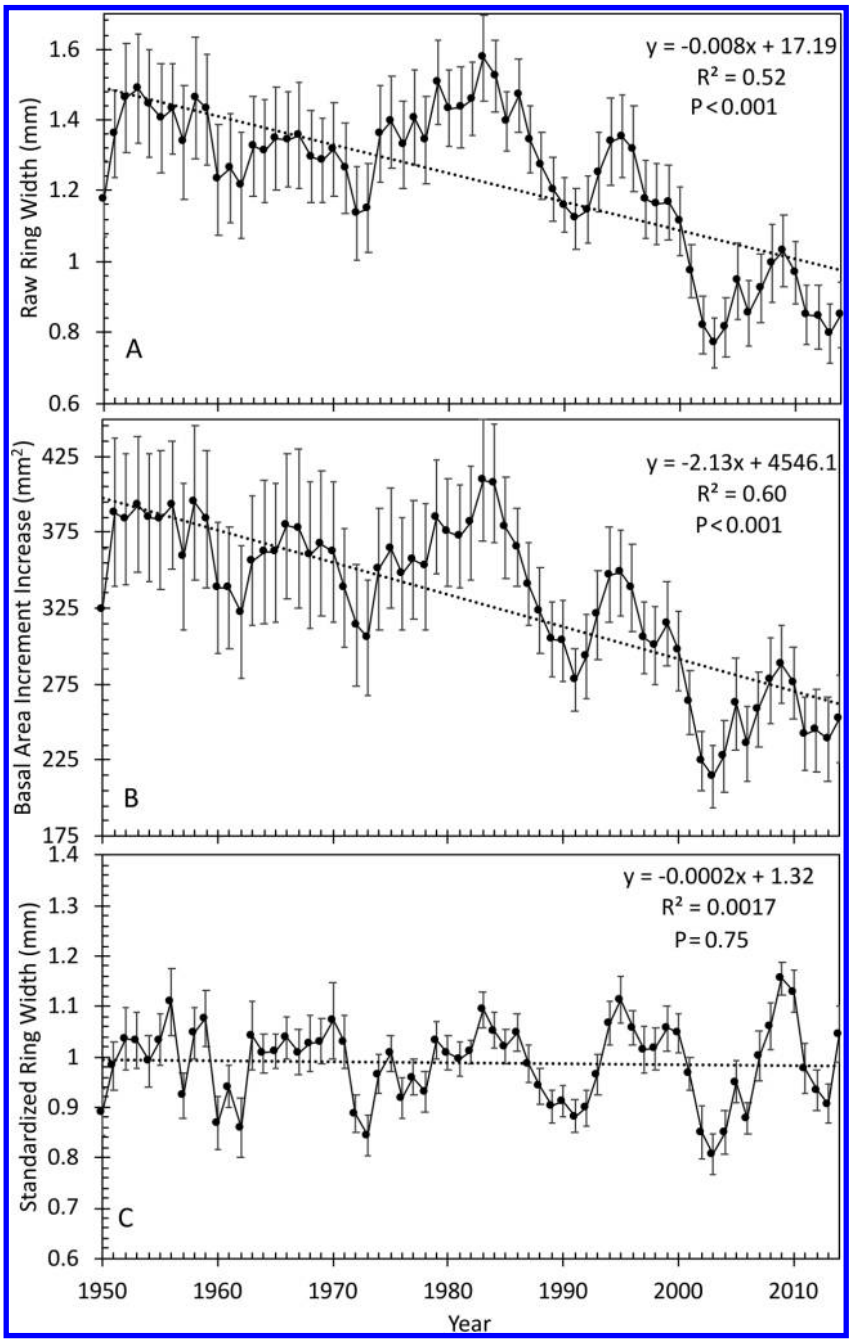

with a long-term average of 0.9 ± 0.3. During the study period, annual PDSI exhibited an upward (wetting) trend, which was significant at $P < 0.1$ ($P = 0.054$) (Fig. 3). Despite this wetting trend, years of moderate to severe droughts were common and constituted around 32% of the 65-year period of study.

Average annual air temperature was 8.9 ± 0.1 °C (Fig. 2), with January mean temperature ranging between –15.1 and 3.0 °C and showing a slight and statistically significant warming over time ($P < 0.01$). March maximum temperatures ranged between 1.8 and 17.6 °C and displayed a significant decreasing trend ($P = 0.048$; Supplementary Fig. S1[1]). July maximum temperatures ranged between 24.4 and 37.4 °C and did not show an increasing or decreasing trend. July mean temperature met or exceeded 21 °C nearly every year except for 1992 (Supplementary Fig. S1[1]).

3.2. Tree-ring chronologies

Tree diameter was positively and significantly correlated with age (Fig. 4). Raw tree-ring widths averaged 1.21 ± 0.02 mm·year⁻¹, and basal area increment (BAI) increase averaged 325.3 ± 4.27 mm²·year⁻¹ (Fig. 5). Both raw tree-ring widths and BAI exhibited a significant decline in growth over time ($P < 0.001$). This decrease can be attributed to the normal growth behavior of *B. papyrifera* in general, as

[1]Supplementary material is available with the article through the journal Web site at http://nrcresearchpress.com/doi/suppl/10.1139/cjfr-2018-0206.

growth is rapid for the first 30 years or so and then sharply declines through maturity (Burns and Honkala 1990). Additionally, as a tree ages, cambial tissue must be distributed over a greater surface area, which results in narrower rings, i.e., the geometrical age effect (Sillett et al. 2015). Data standardization resulted in the removal of any significant trends ($P = 0.74$) and indicated variability around the mean (0.99 ± 0.006 mm), which reflected inter- and intra-annual fluctuations in the abiotic environment (Fig. 5). A decline in tree-ring growth rate was observed in six periods (early 1960s, mid-1970s, late 1980s, early 1990s, early 2000s, and in 2012). These reductions in growth were associated with near-zero or negative (drought) annual PDSI or in years with lower than average air temperatures. Above-average tree-ring widths, standardized ring widths, and BAI were observed during wet years or positive PDSI (e.g., 1983, 1995, and 2009).

3.3. Climate correlations

Previous- and current-year summer and fall streamflow were positively correlated with raw tree-ring widths, BAI, and standardized ring widths (Fig. 6). Generally, streamflow of the previous July through fall of the current year was significantly correlated with standardized tree-ring widths. High precipitation and streamflow rates during April of the current and previous years seemed to have a negative effect on tree-ring growth. Increased air temperatures of both current and previous years were generally negatively correlated with all measured tree parameters, with few exceptions (Fig. 6). The strongest predictor for standardized tree-ring width was PDSI, with values that were significantly and positively correlated at $P < 0.05$ for both the previous and current years. Linear mixed modeling (LMM) highlighted the importance of mid-season water availability of both previous and current years, early season temperature of the current year, and late season temperature of both the previous and current years for tree-ring growth.

3.4. Comparison of climate correlation and LMM

The standardized ring-width model was the most relevant for our study. This model indicated only a negative influence of previous November precipitation on growth, while the R^2 showed significant positive correlation with previous October and December precipitation (Supplementary Table S2[1]). Pearson's R^2 correlations were significantly ($P < 0.05$) negative for previous January and positive for current June, October, and November. Standardized tree-ring widths indicated a disagreement where the model showed late previous season precipitation as negatively impacting growth, while the Pearson R^2 showed significant positive correlation to late season precipitation of both the previous and current years. The LMM and climate correlations all considered virtually the same pool of variables yet produced slightly different results, while the overall results were similar. When using backwards selection, one must reconsider that variables can be dropped early in the model creation process, which could later show significance. One must also consider the overall model as a whole and interpret its meaning within the ecological context of the data itself.

Temperature results from the LMM and Pearson R^2 were in general agreement. Increasing temperatures in previous April and June showed significant negative correlation to standardized ring growth. The findings portrayed from the LMMs and Pearson R^2 correlations were that increasing winter and spring temperatures are unfavorable for growth while increasing summer temperatures are favorable in the absence of drought.

3.5. NDVI as a proxy for vegetation and *B. papyrifera* health

Vegetation composition adjacent to *B. paryrifera* stands were sampled for both ground-truthing and to identify the vegetation, topography, and management practices that would provide the highest correlation with tree rings (Fig. 7). Sampled plots were dominated by grasses (31.9% to 49% cover), averaging 37.6% ± 0.9%. Forbs percent cover ranged between 5.4% and 20.7% and averaged 11.5% ± 0.5%. Shrub percent cover ranged between 6.2% and 27.4% and averaged 17.8% ± 1.1%. Litter percent cover ranged between 36.7% and 67.2% and averaged 52.4% ± 1.5%. Litter composition was significantly lower in plot 4 (38.4%) and plot 7 (36.1%) relative to the others. Standing dead vegetation percent cover averaged 6.2% ± 0.5%. Bare ground percent cover ranged between 28.8% and 54.5% and averaged 41.8% ± 1.5%. Bare ground cover was significantly high in plots 4 (54%), 5 (54%), and 7 (53%) relative to others. Canopy height ranged between 26.9 and 41.6 cm and averaged 34.0 ± 1.4 cm (Fig. 7).

Landsat maximum-value NDVI from all vegetation plots followed the standardized tree-ring growth trend of *B. papyrifera* (Fig. 8; Supplementary Fig. S4[1]). Average Pearson's R^2 correlation values ranged between 0.36 and 0.76. Plot-level correlation was highest in plot 2 for standardized ring width at 0.76 and lowest in plot 8 at 0.36. Regressing standardized ring widths as a function of maximum NDVI values derived from Landsat showed the highest correlation with R^2 of 0.81 (Fig. 9). A notable significant drop in Landsat maximum-value NDVI was observed in 2002. Climate records indicate this year as one of low precipitation, low streamflow, warm temperature, and drought, along with decreased ring growth from the collected *B. papyrifera* dendrochronological record. MODIS summed-value NDVI for the periods of July, August, and August–October reflect the same notable drop in 2002 NDVI for all eight plot locations as seen in the Landsat maximum-value NDVI (data not shown).

The correlation rasters were made semi-transparent and overlain on a triangulated irregular network (TIN, representative of the topographical characteristics of the land) representation of topography, which allowed us to observe any relationship between topography and (or) vegetation composition as characteristics for identifying other sites of comparative use. Based on R^2 values and vegetation communities within the eight sampled plots on the Nature Conservancy property, there was no obvious link between vegetation type and NDVI correlation to ring growth, as plots that contained significant differences of population composition typically showed a lower mean R^2 value (e.g., Supplementary Fig. S4[1]). However, topography similar to that of *B. papyrifera* seemed to play a significant role in identifying the proxy; plots 2, 6, 5, and 3 are all located on rougher areas of the landscape with greater variations in topographical relief and comprised the top half of mean R^2 values of standardized ring width to pixel-level Landsat maximum-value NDVI. Plots 4, 7, 1, and 8 were located on flatter ground and comprised the bottom half of R^2 values of standardized ring width to pixel-level Landsat maximum-value NDVI (Supplementary Figs. S3 and S4[1]). This observed topographical influence appeared to be unrelated to aspect or direction, rather better characterized by the land contour of the general area in question. MODIS summed-value NDVI showed the strongest relationships during July to both raw and standardized growth and during June–August to standardized growth, and there was a consistency of the higher mean-correlated vegetation sampling plots and rough topography, which mostly agrees with the Landsat maximum-value NDVI results at the plot level (correlations are not shown; Supplementary Fig. S3[1]).

Pixel-level correlation of raw tree-ring width and standardized tree-ring width between Landsat maximum-value NDVI and MODIS summed-value NDVI during the summer months showed very similar results when compared with topography and plot-level vegetation composition (Supplementary Figs. S2 and S3[1]).

4. Discussion

Annual average precipitation, temperature, and summer (July) temperature have remained reasonably stable with no upward or downward trends over the study period. However, the area did

Fig. 6. Pearson R^2 correlation of tree-ring width (Raw), basal area increment increase (BAI), and standardized tree ring growth (Std) of *B. papyrifera* as a function of previous- and current-year precipitation, streamflow, temperature, and PDSI along the Niobrara River Valley, Nebraska, between 1950 and 2014. *, significance at $P < 0.1$; **, significance at the $P < 0.05$. [Colour version available online.]

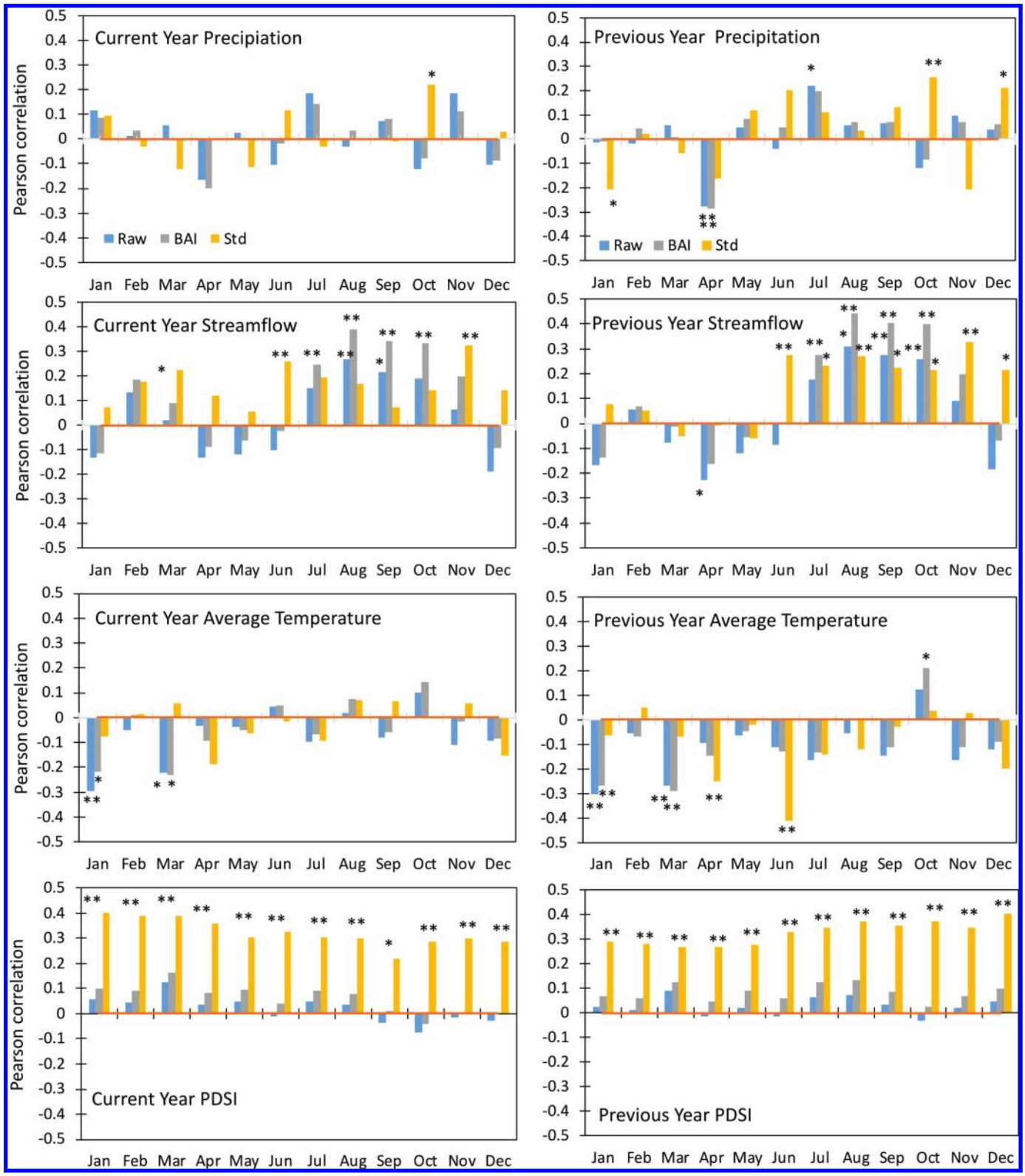

experience a warming trend in January temperature over time (Fig. 2). In northern latitudes, warming winter and spring trends can lead to increased ring growth and treeline advancement into neighboring tundra areas (Kharuk et al. 2014), as well as wider seasonal rings created as a result of earlier bud burst and increased cambial growth associated with a longer growing season (Karlsson et al. 2004; Hollesen et al. 2015; Yang et al. 2017). In this study, we show that warming January air temperatures had a

Fig. 7. Vegetation sampled from eight plots located across a series of management treatments on the Niobrara Valley Preserve, The Nature Conservancy, on 27 June 2016. Each plot consists of an 8 × 6 grid of GPS points (8 east–west, 6 north–south) encompassed in a 640 m × 480 m area. The bar plot on the left shows percent cover of litter, standing dead vegetation, grass, forbs, and bare soil. Map on the right shows the location of the plots relative to sampled trees (white dots). [Colour version available online.]

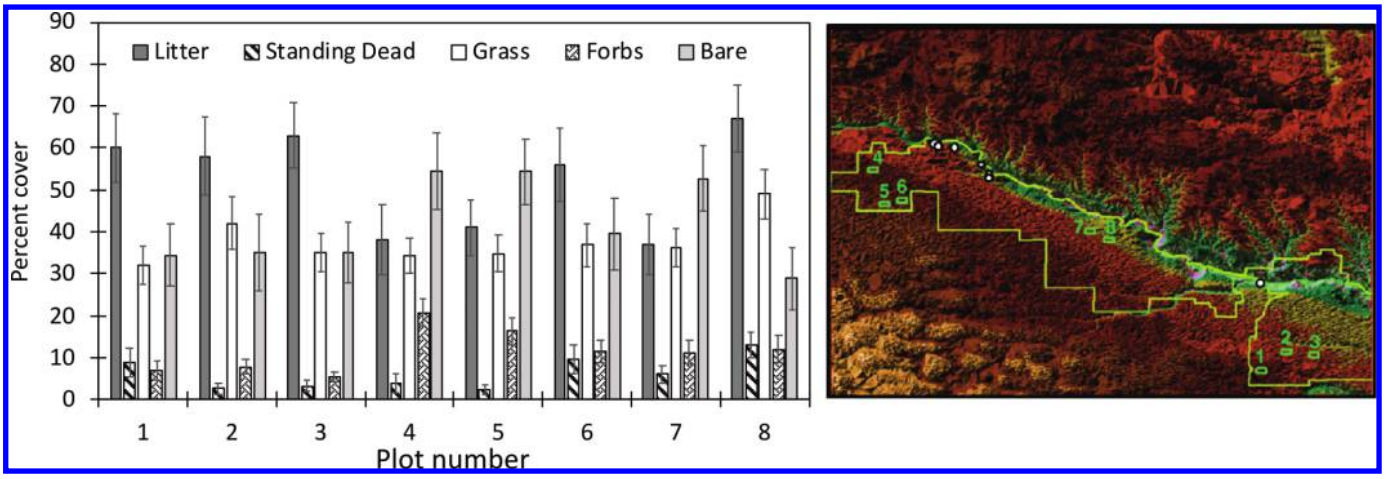

Fig. 8. Average standardized growth of *B. papyifera* and Landsat maximum-value NDVI between 1985 and 2011 within the eight 640 m × 480 m vegetation composition plots sampled in June 2016 by the Nature Conservancy at the Niobrara Valley Preserve in Nebraska. [Colour version available online.]

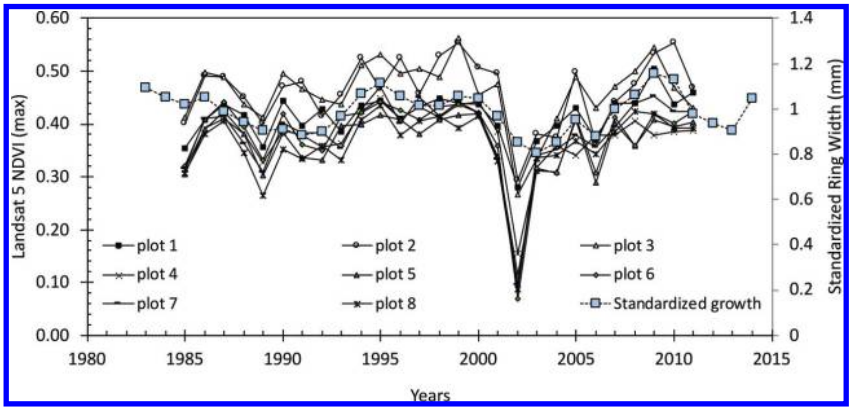

Fig. 9. Standardized ring width of *B. papyrifera* as a function of Landsat maximum-value NDVI observed in adjacent plots in Niobrara River Valley between 1985 and 2011. Missing points are due to cloud cover.

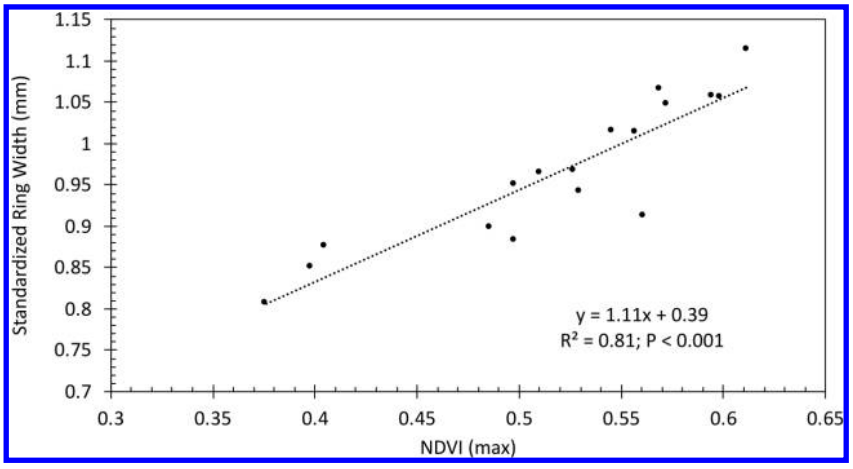

negative effect on growth. This may be due to the higher January minimum temperatures in Nebraska relative to more northern latitudes causing the species to cross a threshold and (or) to re-freezing of the roots, which can ultimately lead to reduction in growth, tree damage (Greenidge 1953; Redmond 1955), or in some cases death (Pomerleau 1991). Water availability has also been shown to have a mixed effect on growth in that its availability encourages establishment and growth of birch species (Li et al. 2016), while water excess (i.e., waterlogged soil) or drought have been shown to decrease leaf area of birch species (Wang et al.

2016). Such may be the case here as the standardized model highlights a negative growth effect from increased precipitation during previous November and current May or late previous and early current seasons. The defoliation response to excess water may very well translate into problematic bud formation in the previous season and bud burst in the following spring. Standardized tree-ring widths followed PDSI very closely, which suggests that inter- and intra-annual growth of *B. papyrifera* is strongly dependent on a combination of temperature and water availability in that warm and wet conditions during the growing season facilitate more growth (Li et al. 2016). This can also be seen notably by the rapid reductions in standardized ring width during years of low (dry) PDSI in the late 1980s to early 1990s and the early 2000s versus an increase in standardized growth during years of high (wet) PDSI in the early 1980s, mid-1990s, and late 2000s, which agrees with other studies (Karlsson et al. 2004; Li et al. 2016). Drought extremes are expected to increase in frequency and duration for the future of the Great Plains (Bathke et al. 2014), which may impact the health and performance of this remnant forest.

Climate correlations showed streamflow from April through November of both previous and current years to be significantly and positively related to growth, agreeing with the inclusion of August streamflow of both current and previous years but disagreeing with the negative influence of July streamflow to raw growth and BAI as displayed by the selected models (Supplementary Table S2[1]). This influence of streamflow on growth might be explained by some of the unique geology of the Niobrara River Valley in that the river water, which flows directly over bedrock, is fed by lateral (easterly) movement of groundwater (Szilagyi et al. 2003). We observed *B. papyrifera* only growing in close proximity to the water's edge in small pockets (Supplementary Table S1[1]). Combining the shallow fibrous root system of paper birch and the influence of drought-related conditions on growth, close proximity of this species to the water table and access to precipitation water or streamflow are necessary for its success.

NDVI values derived from satellite imagery via both Landsat and MODIS satellites showed potential use as a proxy for ex situ *B. papyrifera* growth monitoring through high Pearson's R^2 values between ring growth and NDVI at the pixel level. Based on R^2 values and vegetation communities within the eight sampled plots, there was no obvious link between vegetation type and NDVI correlation to tree-ring growth. However, vegetation on topography, similar to that of *B. papyrifera*, played a significant role in identifying the proxy. Other studies have linked satellite NDVI to climate variables such as temperature, precipitation, and drought conditions (Baird et al. 2012; Jia et al. 2003) and tree-ring width to NDVI with mixed success (Coops et al. 1999; Forbes et al. 2010; Vicente-Serrano et al. 2016). For example, Bhuyan et al. (2017) noted a positive relationship between NDVI and tree rings in many forests in the Northern Hemisphere; however, the strength of this relationship depended on spatial scale, forest type (e.g., better correlation of NDVI with tree rings of conifers than deciduous species), species phenology, climatic zones, and method of combining NDVI for analysis. Liang et al. (2005) reported strong relationship between grasslands NDVI and *Picea meyeri* in the semi-arid region of northern China. They argued that in semi-arid regions, such relationships can be expected as both vegetation types are limited by seasonal precipitation. Similarly, in this study, where water is a limiting factor, we found that using NDVI of adjacent pasture lands with similar topographical characteristics to that of *B. papyrifera* can provide a reliable representation of tree performance.

5. Conclusion

Dendrochronological techniques were used to identify microclimatic drivers of *B. papyrifera* growth of the Niobrara River Valley. We found intra- and inter-annual averages and patterns of precipitation, temperature, streamflow, and PDSI to be important for predicting growth. Climate correlations and LMM analyses produced similar results with some disagreements but with both methods agreeing that the strongest predictor for standardized tree rings was the PDSI, suggesting that *B. papyrifera* is highly responsive to a combination of temperature and water. Increasing winter and spring temperatures were unfavorable for tree growth, while increasing summer temperatures were favorable in the absence of drought. Drought is expected to increase in frequency and duration for the future of the Great Plains (Bathke et al. 2014). Warming conditions are also expected in the northern latitudes (Soja et al. 2007) and have been shown to impact riparian ecosystems, leading to decreased biomass of riparian species and overall species richness and diversity. Riparian communities that depend on groundwater are predicted to be replaced with more water-competitive upland communities (Ström et al. 2011). Combining the shallow fibrous root system of *B. papyrifera* and the influence of drought-related conditions on growth, the future of *B. papyrifera* of the Niobrara River Valley will be dependent on climate and water availability at key points during the growing season. Factors such as water pumping for irrigation purposes on upland sites and expansion of woody species, especially the encroachment of *Juniperus virginiana* (Awada et al. 2013), will affect the horizontal movement of water over bedrock and impact water availability for *B. papyrifera* and should therefore be monitored.

High NDVI values derived from satellites images of adjacent grasslands correlated with *B. papyrifera*, indicating that vegetation that shares the same topographic relief is governed by similar environmental constraints in semi-arid areas (i.e., water) and can be used as a proxy to monitor a sparsely populated and (or) remote species growth ex situ. Results from this study can aid in forecasting the dynamics and thresholds of this species in the face of climate change in both the remnant populations and across its current distribution in northern latitudes of North America.

Acknowledgement

This study was supported by the McIntire Stennis Forest Research Funds, U.S. Department of Agriculture. The authors would like to thank the staff of the Dendrochronology Laboratory of the Swiss Federal Institute for Forests, Snow and Landscape for their assistance with the tree-ring samples. We thank the High Plains Regional Climate Center (HPRCC, University of Nebraska-Lincoln) for the climate data, Les Howard for creating the location map, and the Nebraska Nature Conservancy and its staff for providing access to the Niobrara Valley Preserve and data on upland sites. We are also grateful for the two anonymous reviewers for their comments on the manuscript.

References

Aus Der Au, R., Awada, T., Battipaglia, G., Hiller, J., Saurer, M., and Cherubini, P. 2018. Tree rings of *Pinus ponderosa* and *Juniperus virginiana* show different responses to stand density and water availability in the Nebraska grasslands. Am. Midl. Nat. **180**: 18–37. doi:10.1674/0003-0031-180.1.18.

Awada, T., El-Hage, R., Geha, M., Wedin, D.A., Huddle, J.A., Zhou, X., Msanne, J., Sudmeyer, R.A., Martin, D.L., and Brandle, J.R. 2013. Intra-annual variability and environmental controls over transpiration in a 58-year-old even-aged stand of invasive woody *Juniperus virginiana* L. in the Nebraska Sandhills, USA. Ecohydrology, **6**: 731–740. doi:10.1002/eco.1294.

Baird, R.A., Verbyla, D., and Hollingsworth, T.N. 2012. Browning of the landscape of interior Alaska based on 1986–2009 Landsat sensor NDVI. Can. J. For. Res. **42**(7): 1371–1382. doi:10.1139/x2012-088.

Bates, D., Mächler, M., Bolker, B., and Walker, S. 2015. Fitting linear mixed-effects models using lme4. J. Stat. Softw. **67**: 1–48. doi:10.18637/jss.v067.i01.

Bathke, D.J., Oglesby, R.J., Rowe, C.M., and Wilhite, D.A. 2014. Understanding and assessing climate change: implications for Nebraska. University of Nebraska Press, Lincoln, Nebraska.

Bhuyan, U., Zang, C., Vicente-Serrano, S.M., and Menzel, A. 2017. Exploring relationships among tree-ring growth, climate variability, and seasonal leaf activity on varying timescales and spatial resolutions. Remote Sens. **9**: 526. doi:10.3390/rs9060526.

Bradley, E. 1956. Geology and ground-water resources of the upper Niobrara River Basin, Nebraska and Wyoming. U.S. Geological Survey, Water Supply Paper 1368. doi:10.3133/wsp1368.

Bunn, A.G., Hughes, M.K., Kirdyanov, A.V., Losleben, M., Shishov, V.V., Berner, L.T., Oltchev, A., and Vaganov, E.A. 2013. Comparing forest measurements from tree rings and a space-based index of vegetation activity in Siberia. Environ. Res. Lett. **8**: 035034. doi:10.1088/1748-9326/8/3/035034.

Burnham, K.P., and Anderson, D.R. 2002. Model selection and multimodel inference: a practical information-theoretical approach. 2nd ed. Springer-Verlag, New York. doi:10.1007/b97636.

Burns, R.M., and Honkala, B.H. 1990. Silvics of North America. USDA Forest Service, Washington, D.C., Agric. Handb. No. 654.

Cady, R.C., and Scherer, O.J. 1946. Geology and ground-water resources of Box Butte County, Nebraska. U.S. Geological Survey, Water Supply Paper 969. doi:10.3133/wsp969.

Campelo, F. 2012. DetrendeR: start the detrendeR graphical user interface (GUI) [online]. R package version 1.0.4. Available from https://CRAN.R-project.org/package=detrendeR.

Cherubini, P., Fontana, G., Rigling, D., Dobbertin, M., Brang, P., and Innes, J.L. 2002. Tree-life history prior to death: two fungal root pathogens affect tree-ring growth differently. J. Ecol. **90**: 839–850. doi:10.1046/j.1365-2745.2002.00715.x.

Cook, E.R., and Holmes, R.L. 1986. Users' manual for program ARSTAN. Laboratory of Tree-Ring Research, University of Arizona, Tucson, Ariz.

Coops, N., Bi, H., Barnett, P., and Ryan, P. 1999. Estimating mean and current annual increments of stand volume in a regrowth eucalypt forest using historical Landsat multi spectral scanner imagery. J. Sustainable For. **9**(3–4): 149–168. doi:10.1300/J091v09n03_07.

Di Matteo, G., De Angelis, P., Brugnoli, E., Cherubini, P., and Scarascia-Mugnozza, G. 2010. Tree-ring $\Delta^{13}C$ reveals the impact of past forest management on water-use efficiency in a Mediterranean oak coppice in Tuscany (Italy). Ann. For. Sci. **67**: 510. doi:10.1051/forest/2010012.

Eckstein, D., and Bauch, J. 1969. Beitrag zur Rationalisierung eines Dendrochronologischen Verfahrens und zur Analyse seiner Aussagesicherheit. Forstwirtschaftliches Zentralblatt, 88. Verlag Paul Parey, Hamburg.

Forbes, B.C., Fauria, M.M., and Zetterberg, P. 2010. Russian Arctic warming and 'greening' are closely tracked by tundra shrub willows. Glob. Change Biol. **16**: 1542–1554. doi:10.1111/j.1365-2486.2009.02047.x.

Fowells, H.A. (*Editor*). 1965. Silvics of forest trees of the United States. USDA Forest Service, Washington, D.C., Agric. Handb. No. 271.

Greenidge, K.N.H. 1953. Further studies of birch dieback in Nova Scotia. Can. J. Bot. **31**(5): 548–559. doi:10.1139/b53-044.

Grissino-Mayer, H.D. 2001. Evaluating crossdating accuracy: a manual and tutorial for the computer program COFECHA. Tree-Ring Res. **57**: 205–221.

He, J., and Shao, X. 2006. Relationships between tree-ring width index and NDVI of grassland in Delingha. Chin. Sci. Bull. **51**: 1106–1114. doi:10.1007/s11434-006-1106-4.

Hollesen, J., Buchwal, A., Rachlewicz, G., Hansen, B.U., Hansen, M.O., Stecher, O., and Elberling, B. 2015. Winter warming as an important co-driver for *Betula nana* growth in western Greenland during the past century. Glob. Change Biol. **21**: 2410–2423. doi:10.1111/gcb.12913.

Jia, G.J., Epstein, H.E., and Walker, D.A. 2003. Greening of arctic Alaska, 1981–2001. Geophys. Res. Lett. **30**(20). doi:10.1029/2003GL018268.

Karlsson, P.S., Tenow, O., Bylund, H., Hoogesteger, J., and Weih, M. 2004. Determinants of mountain birch growth in situ: effects of temperature and herbivory. Ecography, **27**: 659–667. doi:10.1111/j.0906-7590.2004.03869.x.

Kharuk, V.I., Kuzmichev, V.V., Im, S.T., and Ranson, K.J. 2014. Birch stands growth increase in western Siberia. Scand. J. For. Res. **29**: 421–426. doi:10.1080/02827581.2014.912345.

Kumar, L., and Mutanga, O. 2017. Remote sensing of above-ground biomass. Remote Sens. **9**: 935. doi:10.3390/rs9090935.

Li, B., Heijmans, M.M.P.D., Berendse, F., Blok, D., Maximov, T., and Sass-klaassen, U. 2016. The role of summer precipitation and summer temperature in establishment and growth of dwarf shrub *Betula nana* in Northeast Siberian Tundra. Polar Biol. **39**: 1245–1255. doi:10.1007/s00300-015-1847-0.

Li, L., Guo, Q., Tao, S., Kelly, M., and Xu, G. 2015. LiDAR with multi-temporal MODIS provide a means to upscale predictions of forest biomass. ISPRS J. Photogram. Remote Sens. **102**: 198–208. doi:10.1016/j.isprsjprs.2015.02.007.

Liang, E.Y., Shao, X.M., and He, J.C. 2005. Relationships between tree growth and NDVI of grassland in the semi-arid grassland of north China. Int. J. Remote Sens. **26**: 2901–2908. doi:10.1080/01431160500056931.

Maeglin, R.R. 1979. Increment cores: how to collect, handle and use them. USDA Forest Products Laboratory, Madison, Wisconsin, Gen. Tech. Rep. FPL-25.

Pomerleau, R. 1991. Experiments on the causal mechanisms of dieback on deciduous forests in Quebec. Forestry Canada, Quebec Region, Sainte-Foy, Que., Can. For. Serv. Inf. Rep. LAU-X-96.

Redmond, D.R. 1955. Studies in forest pathology: XV. Rootlets, mycorrhiza, and soil temperature in relation to birch dieback. Can. J. Bot. **33**(6): 595–627. doi:10.1139/b55-048.

Reed, B.C., Loveland, T.R., and Tieszen, L.L. 1996. An approach for using AVHRR data to monitor U.S. Great Plains grasslands. Geocarto Int. **11**: 13–22. doi:10.1080/10106049609354544.

Rinn, F. 2003. TSAP-Win: time series analysis and presentation for dendrochronology and related applications [online]. Version 0.55 user reference. Heidelberg, Germany.

Schweingruber, F.H. 1996. Tree rings and environment: dendroecology. Paul Haupt AG Bern, Berne, Switzerland.

Sillett, S.C., Van Pelt, R., Carroll, A.L., Kramer, R.D., Ambrose, A.R., and Trask, D. 2015. How do tree structure and old age affect growth potential of California redwoods? Ecol. Monogr. **85**: 181–212. doi:10.1890/14-1016.1.

Soja, A.J., Tchebakova, N.M., French, N.H.F., Flannigan, M.D., Shugart, H.H., Stocks, B.J., Sukhinin, A.I., Parfenova, E.I., Chapin, S.F., III, and Stackhouse, P.W., Jr. 2007. Climate-induced boreal forest change: predictions versus current observations. Glob. Planet. Change, **56**: 274–296. doi:10.1016/j.gloplacha.2006.07.028.

Statistical Consulting Group (UCLA). 2006. Introduction to generalized linear mixed models [online]. University of California, Los Angeles (UCLA). Available from http://stats.idre.ucla.edu/other/mult-pkg/introduction-to-generalized-linear-mixed-models [accessed 15 September 2017].

Stokes, M.A., and Smiley, T.L. 1968. An introduction to tree-ring dating. University of Arizona Press, Tucson, Ariz.

Stroh, E.D., and Miller, J.P. 2009. Paper birch decline in the Niobrara River Valley, Nebraska: weather, microclimate, and birch stand conditions. U.S. Geological Survey, Open-File Report 2009–1221. doi:10.3133/ofr20091221.

Ström, L., Jansson, R., Nilsson, C., Johansson, M.E., and Xiong, S. 2011. Hydrologic effects on riparian vegetation in a boreal river: an experiment testing climate change predictions. Glob. Change Biol. **17**: 254–267. doi:10.1111/j.1365-2486.2010.02230.x.

Szilagyi, J., Harvey, F.E., and Ayers, J.F. 2003. Regional estimation of base recharge to ground water using water balance and a base-flow index. Ground Water, **41**: 504–513. doi:10.1111/j.1745-6584.2003.tb02384.x. PMID:12873013.

Vicente-Serrano, S.M., Camarero, J.J., Olano, J.M., Martín-Hernández, N., Peña-Gallardo, M., Tomás-Burguera, M., Gazol, A., Azorin-Molina, C., Bhuyan, U., and El Kenawy, A. 2016. Diverse relationships between forest growth and the normalized difference vegetation index at a global scale. Remote Sens. Environ. **187**: 14–29. doi:10.1016/j.rse.2016.10.001.

Wang, A.F., Roitto, M., Sutinen, S., Lehto, T., Heinonen, J., Zhang, G., and Repo, T. 2016. Waterlogging in late dormancy and the early growth phase affected root and leaf morphology in *Betula pendula* and *Betula pubescens* seedlings. Tree Physiol. **36**: 86–98. doi:10.1093/treephys/tpv089. PMID:26420790.

Wright, H.E., Jr. 1970. Vegetational history of the central plains. *In* Pleistocene and recent environments of the Central Great Plains. *Edited by* W. Dort, Jr. and J.K. Jones, Jr. University of Kansas Press, Lawrence, Kansas. pp. 157–172.

Yang, B., He, M., Shishov, V., Tychkov, I., Vaganov, E., Rossi, S., Ljungqvist, F.C., Bräuning, A., and Grießinger, J. 2017. New perspective on spring vegetation phenology and global climate change based on Tibetan plateau tree-ring data. Proc. Natl. Acad. Sci. U.S.A. **114**: 6966–6971. doi:10.1073/pnas.1616608114. PMID:28630302.